SIMULATIONS OF ELECTRON-PROTON BEAM INTERACTION BEFORE PLASMA IN THE AWAKE EXPERIMENT

U. Dorda, R. Assmann, J. Grebenyuk, DESY, Hamburg, Germany
C. Bracco, A. Petrenko, J. Schmidt, CERN, Geneva, Switzerland

Abstract

The on-axis injection of electron bunches in the proton-driven plasma wake at the AWAKE experiment at CERN implies co-propagation of a low-energy electron beam with the long high-energy proton beam in a common beam pipe over several meters upstream of the plasma chamber. The possible effects of the proton-induced wakefields on the electron bunch phase space in the common beam pipe region may have crucial implications for subsequent electron trapping and acceleration in plasma. We present the PIC simulations with CST Studio as well as direct-beam-beam interaction simulations of the tentative common beam pipe setup and the two beam co-propagating in it.

INTRODUCTION

The AWAKE experiment is a proof-of-principle experiment that aims to utilize the 400 GeV proton beam from the SPS to drive a plasma-wake allowing to accelerate electrons from a few MeV to the GeV scale within a single plasma stage of a few meter length [1]. For this purpose a low-energy electron beam is bent onto the high-energy proton beam trajectory a few meters upstream of the plasma chamber (Figure 1) [2]. This paper reports on studies performed on the effect (wake fields and direct beam-beam interaction) of the proton beam on the electron beam over these few meters of common vacuum chamber. In this section, the common beam pipe is circular with a default diameter of d = 60 mm up to 1 m before the start of the plasma chamber where it's diameter is reduced to d = 40 mm (Assumed thickness: 2 mm, conductivity: 7.7E6 S/m). This common section is equipped with several quadrupoles allowing to focus the electron beam at the plasma entrance, corrector magnets and beam diagnostic devices [3]. In the foreseen

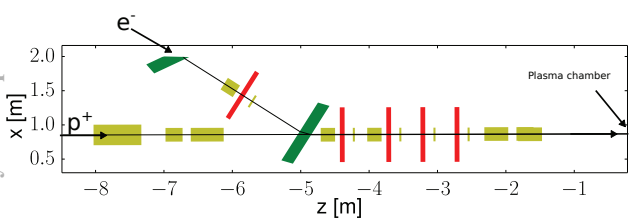

Figure 1: Sketch of the layout upstream of the plasma chamber where the high energy proton and low energy electron beam co-propagate (green: dipoles, red: quadrupoles, yellow: orbit correctors & beam diagnostic devices).

default operation scenario, the arrival of the two beams is adjusted to position the short electron beam slightly behind the center of the significantly longer proton bunch. To be on the safe side and to anticipate experimental modifications, a centered electron beam sampling the maximal direct beam-beam force was assumed. Table 1 and Figure 2 list/illustrate the proton and electron beam parameters and optics in this common section.

Table 1: Beam Parameters of the Proton and Electron Beam

Parameter	Protons	Electrons
Energy [GeV]	400	0.016
Nr of particles	3E11	1.2E9
$\epsilon_{n,xy}$ [π mm mrad]	3.5	2.0
Bunch length [1σ, mm]	120	1.2
Momentum spread [10^{-3}]	2.0	5.0
β_x [m]	7.0	1.02
β_y [m]	7.0	5.39

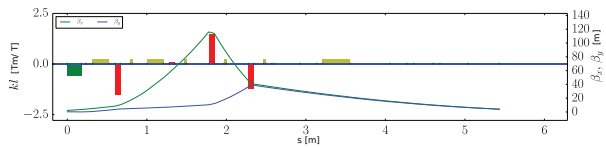

Figure 2: Electron beam optics along the common beam section. The $\beta_{x,y}$ of the proton beam is almost constant at $\approx 7m$.

WAKE FIELD STUDIES WITH CST

The "Particle In Cell" (PIC) - solver of "CST Particle Studio 2014" was used to simulate the interaction between the two beams including wake-fields taking a mock-up geometry of the vacuum chamber into account. The 6D-initial particle distributions (25000 macro-particles electrons, 50000 macro-particle protons) were externally created and imported using the "CST-particle interfaces" feature. In order to reduce the computational effort, the proton beam was cut right after the electron beam. As the two beams are launched at separate locations, the perturbations due to the non-self-consistent initialization are no issue. The fields of the magnets (dipoles and quadrupoles) were imported into CST based on ideal, hard edge models. Due to the large size of the model, special attention had to be put on the choice of mesh-parameters, where a valid compromise between computational feasibility and physical correctness had to be found. While a suitable trade-off could be found to represent the longer distance effects of the wake-fields including the interaction with the vacuum chamber, a separate code based on analytical field-formulas had to be written to study the direct beam-beam interaction at low amplitudes (see next

Copyright © 2015 CC-BY-3.0 and by the respective authors

section). A cross-section of the vacuum chamber model used in the CST simulations is shown in Figure 3.

Figure 3: Cross section view of the simulated vacuum chamber model. The initial particle distributions are shown in green.

Figure 4 shows an example of the magnetic field pattern co-propagating with the two beams just before they are merged. It can be seen that the vacuum chamber effectively shields any magnetic fields.

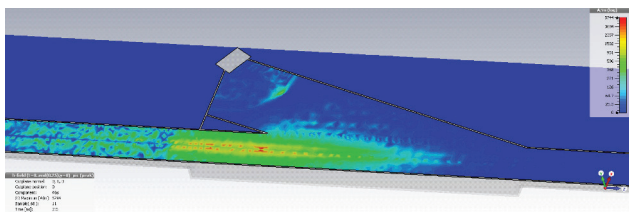

Figure 4: Absolute value of the magnetic field just before the two beams are merged.

The effect on the electron phase-space distribution at the plasma-chamber entrance is illustrated in Figure 5 and 6. In the vertical plane it is clearly visible that the dominant effect is due to the direct beam-beam interaction causing a non-linear detuning with amplitude. In the horizontal plane on the other hand, CSR effects in the merging dipole were identified as the major source of phase-space distortions. The combined effect due to CSR and wakefield results in a phase-space distortion of the beam injected into the plasma-wake field experiment are significant and further optimization of the beam line (additional focusing etc) will be done in the future.

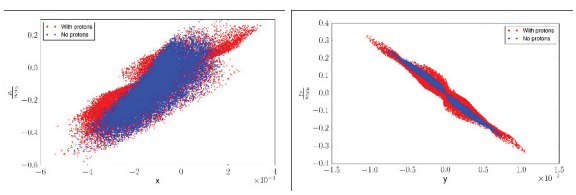

(a) Horizontal phase space (b) Vertical phase space

Figure 5: Electron phase space distortions simulated at the start of the plasma cell (simulated with CST).

DIRECT BEAM-BEAM INTERACTION SIMULATION

Next a dedicated tracking code implementing the direct space charge effect was written to study the details of the direct beam-beam interaction. As this code is based on analytic formulas for the magnetic and electric fields of the proton beam with transverse elliptic Gaussian beam profile [4], it is not subject to numerical resolution limitations. This

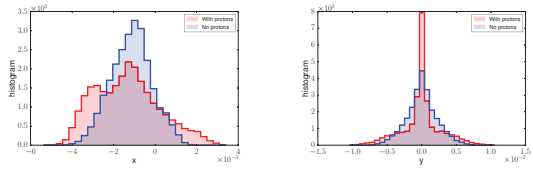

(a) Horizontal (b) Vertical

Figure 6: Histogram of the electron phase space distortions at the start of the plasma cell corresponding to Figure 5 (simulated with CST).

also allowed to simulate a different, newer version of the layout with an increased length of the common beam-pipe section. The great difference in magnetic rigidity of the two beams justifies the usage of a weak-strong model. The dipole and quadrupole are simulated as a sequence of thin lens elements. The various kicks due to the magnets, beam-beam interaction or electron self space charge are affected every 5 mm.

Figure 7 shows the phase space and transverse histogram of the electron beam at the entrance of the plasma chamber for three different proton beam currents. The filamentation due to the nonlinear detuning of the beam-beam interaction, can be clearly seen leading to an emittance blow-up.

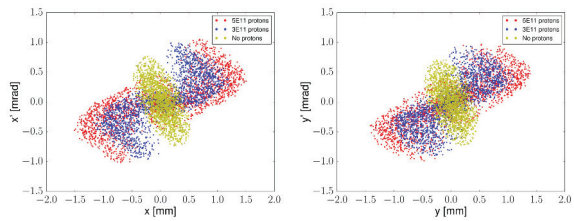

(a) Transverse phase space distribution

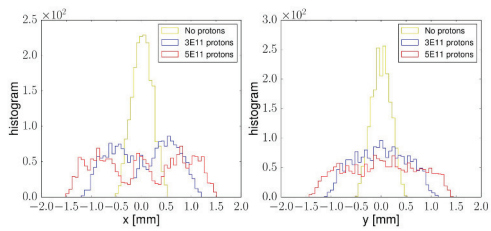

(b) Histograms of the transverse beam profiles

Figure 7: Effect of the beam-beam interaction on the distribution at the entrance of the plasma chamber in case of no, $3 \cdot 10^{11}$ and $5 \cdot 10^{11}$ protons.

The distortions of the phase-space can be clearly identified as a superposition of two extremes (Figure 8): High amplitude particles are on average not significantly affected by the proton-beam while the low-amplitude particles experience an additional focusing quadrupole-like field. The equivalent quadrupole strength per meter is given by

$$K = \frac{eI(1-\beta_e\beta_p)}{2\pi\epsilon_0\beta_p c}\frac{1}{2\sigma^2}\frac{1}{m_{0,e}\gamma_e\beta_e^2 c^2} \quad (1)$$

ISBN 978-3-95450-168-7

Copyright © 2015 CC-BY-3.0 and by the respective authors

In the given configuration this amounts to an equivalent normalized quadrupole strength of K = 0.05.

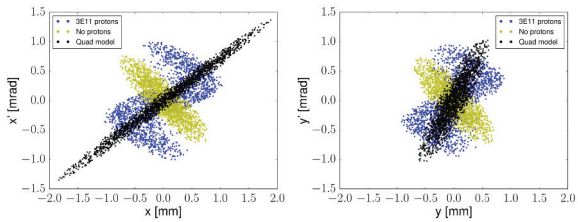

Figure 8: Transverse phase-spaces at the start of the plasma cell in case of a) no proton beam (yellow) b) space charge model (blue) c) equivalent linear focusing (black).

In order to study the sensibility to orbit-excursions and to see if an intentional offset could be used to mitigate the perturbation, the offset-scans following different orbit excursions were performed. Figure 9 shows the effect of a constant offset in the the horizontal plane between the two beams all along the whole common section (which would imply that the magnets are physically shifted) for various different separation distances ($\sigma_{proton} = 0.24mm$). As expected the effect in the vertical plane is limited to a slight reduction of the distortion, while in the horizontal plane the region that is affected is shifted accordingly.

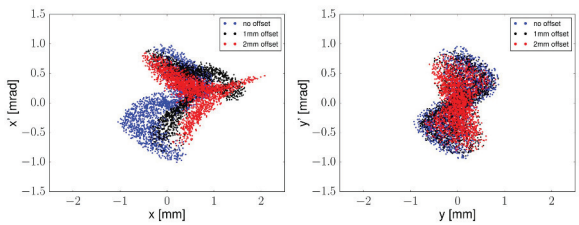

Figure 9: The effect of the direct beam-beam interaction on the transverse phase-space at the start of the plasma cell in case of a constant horizontal offset between the two beams.

More realistically, the quadrupoles would be aligned around the proton beam orbit and the electron beam would be at varying distance to the proton beam [2]. Only the last two correctors upstream of the plasma chamber would be used to finally align the two beams on top of each other. In the simulated case, the electron beam always remained at one side of the proton beam with a maximal distance of 4.5 mm (Figure 10 a). Figure 10-b shows that the resulting mixing of detuning would significantly reduce the perturbations.

By observing the electron beam size after the empty 10 m long plasma section one can check if the beams overlap in space and time correctly (see Figure 11). We note that the properly matched electron beam becomes trapped by the attraction to the proton beam. The beam parameters are symmetric in this case and thus the effect is also identical in both planes.

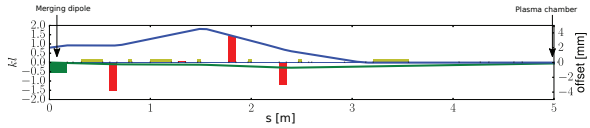

(a) The assumed orbit excursion (blue = horizontal, green = vertical)

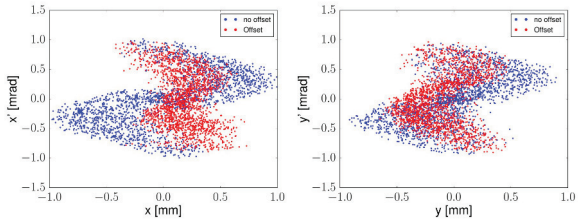

(b) Transverse phase-space at the start of the plasma cell

Figure 10: An intentional orbit offset between the two beams with only the last corrector used to perfectly overlap the two beams, would significantly reduce the phase-space distortions.

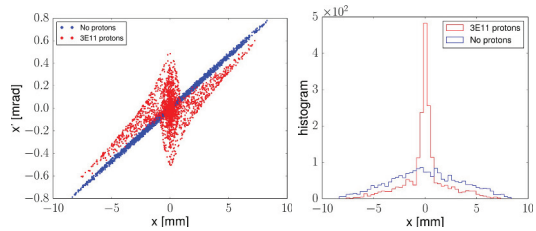

(a) Transverse Phase space (b) Histograms

Figure 11: Operating the plasma chamber without plasma and observing the transverse beam profile at the exit might help to optimize the spacial and temporal overlap of the two beams.

Finally, a simple electron space-charge model based on analytic formulas for the fields of a Gaussian beam was applied and it was confirmed that the additional effect is negligible compared to the beam-beam interaction and no additional emittance blow-up is observed.

CONCLUSION

Full PIC-simulations using CST and dedicated beam-beam studies have been performed illustrating the significance of the collective effects (CSR, wake-field, beam-beam interaction, ...) in the common beam pipe section just upstream of the plasma cell. While we've managed to transport all the electrons and to put them on-axis with the proton beam at the plasma entrance, the observed blow up of the electron beam size would result in a reduced capture efficiency. Therefore improvements like stronger focusing will be studied in the future. The final optimization of the electron beam injection will depend on the details of plasma entrance design, especially on the length of plasma density transition from zero to the constant value.

Copyright © 2015 CC-BY-3.0 and by the respective authors

REFERENCES

[1] R. Assmann et al (AWAKE Collaboration). "Proton-driven plasma wakefield acceleration: A path to the future of high-energy particle physics." Plasma Phys. Control. Fusion 56, 084013 (2014).

[2] J. S. Schmidt et al. "The AWAKE electron primary beam line", These Proceedings, IPAC'15, Richmond, USA (2015).

[3] A. Caldwell, E. Gschwendtner, K. Lotov, P. Muggli, M. Wing, "AWAKE Design Report A Proton-Driven Plasma Wakefield Acceleration Experiment at CERN", CERN-SPSC-2013-013. SPSC-TDR-003, 2013.

[4] M. Bassetti, G.A. Erskine, "Closed expression for the electrical field of a two-dimensional Gaussian Charge", CERN report, CERN-ISR-TH/80-06.

Copyright © 2015 CC-BY-3.0 and by the respective authors

ISBN 978-3-95450-168-7